Supporting Information

Visual temperature-sensing properties of negative thermal expansion $Sc_2Mo_3O_{12}$:Eu^{3+}/Tb^{3+} flexible films

Kan Kan[a]; Yangke Cun[a,†]; Qinghan Zhang[a]; Shenglin Ma[a]; Shilei Yan[a]; Anjun Huang[a]; Zhengwen Yang[a,†];

[a]*College of Materials Science and Engineering, Kunming University of Science and Technology, Kunming, 650093, China;*

[b]*School of Chemistry and Oil and Gas Technology, Kuzbas National Technical University, Kemerovo 650000, Russia*

* *Corresponding author.* （*E-mail: cunyangke@126.com; yangzw@kust.edu.cn*）

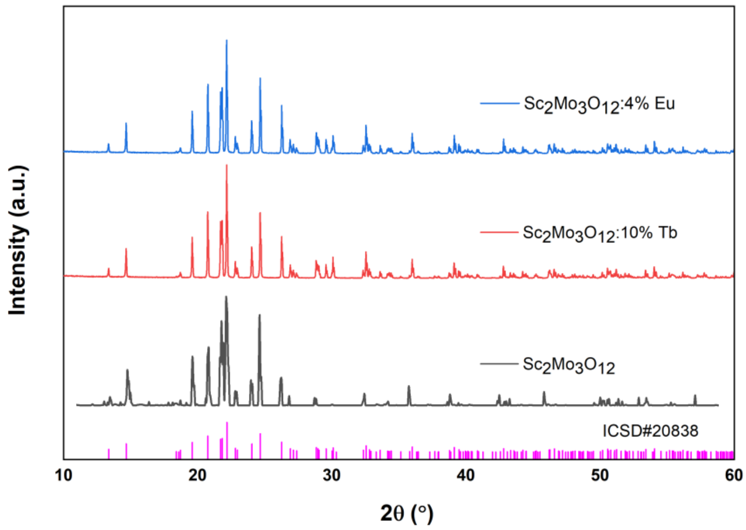

Figure.S1. (Color online) XRD pattern of $Sc_2Mo_3O_{12}$: Tb^{3+} and $Sc_2Mo_3O_{12}$: Eu^{3+} phosphors.

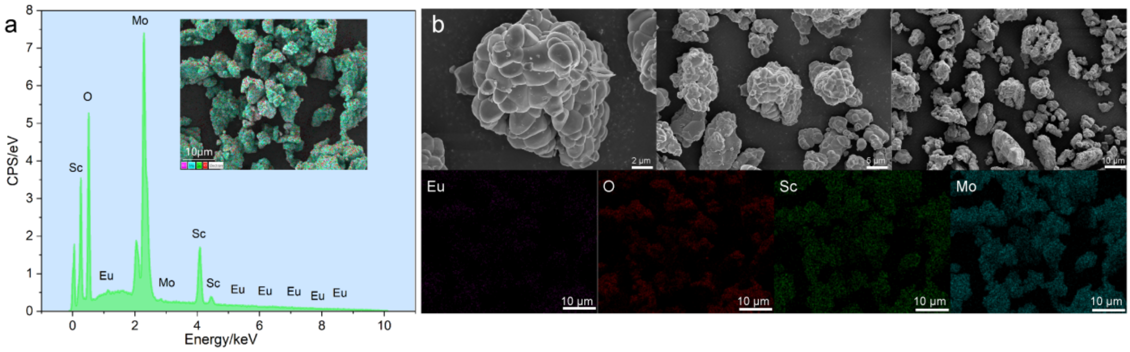

Figure.S2. (Color online) (a) SEM micrograph and (b) EDS elemental analysis of $Sc_2Mo_3O_{12}$: Eu^{3+} phosphors.

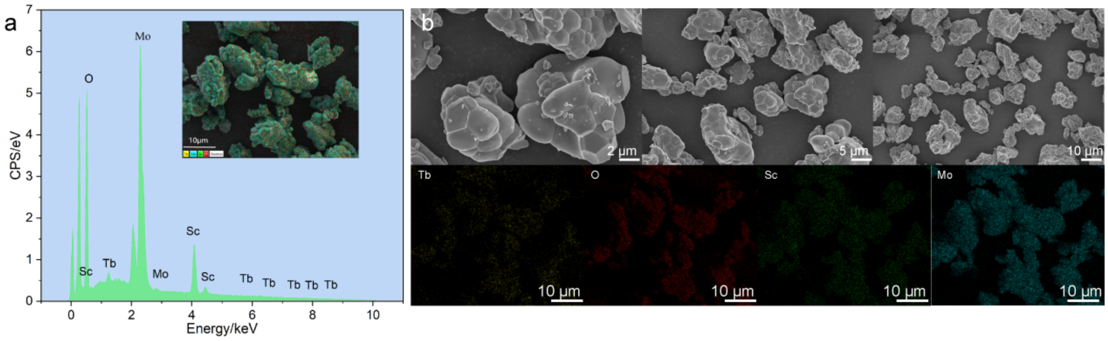

Figure.S3. (Color online) (a) SEM micrograph and (b) EDS elemental analysis of $Sc_2Mo_3O_{12}$: Tb^{3+} phosphors.

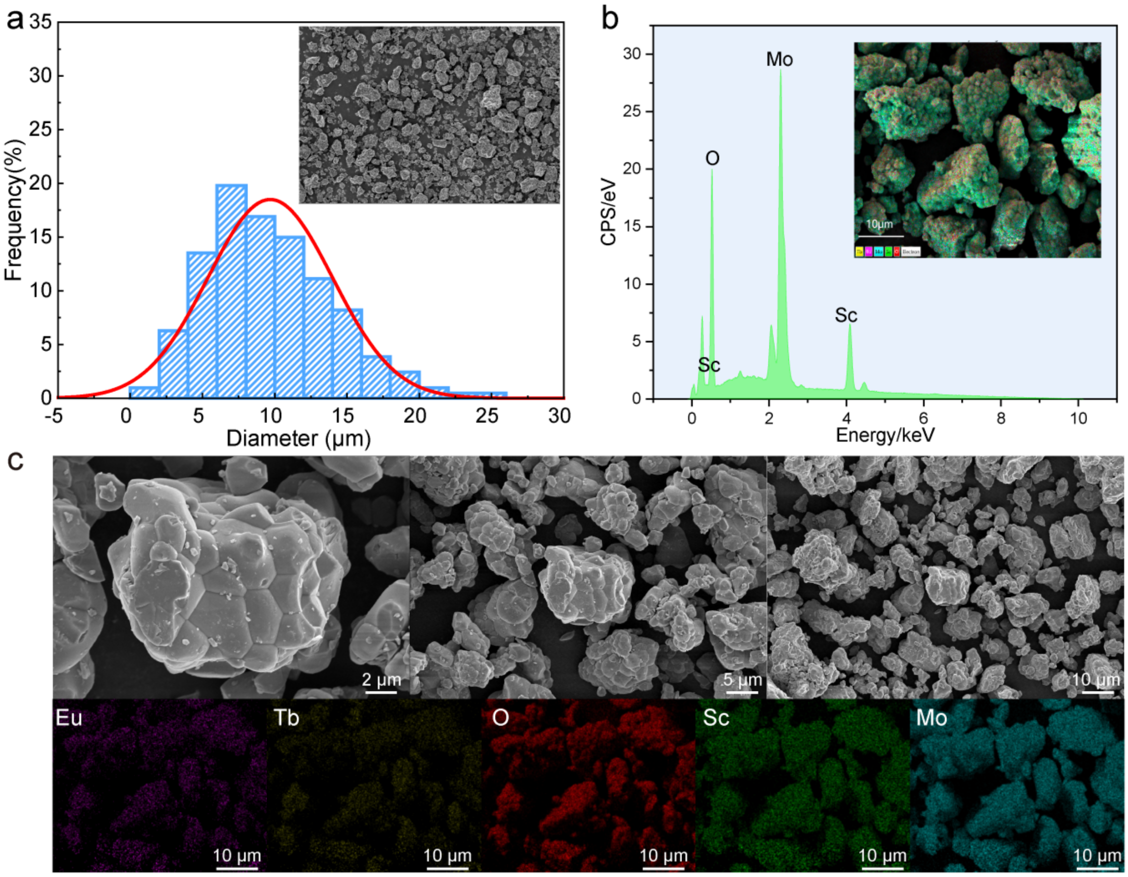

Figure.S4. (Color online) (a) The particle size distribution diagrams, (b) SEM micrograph and (c) EDS elemental analysis of $Sc_2Mo_3O_{12}$: Eu^{3+}/Tb^{3+} phosphors.

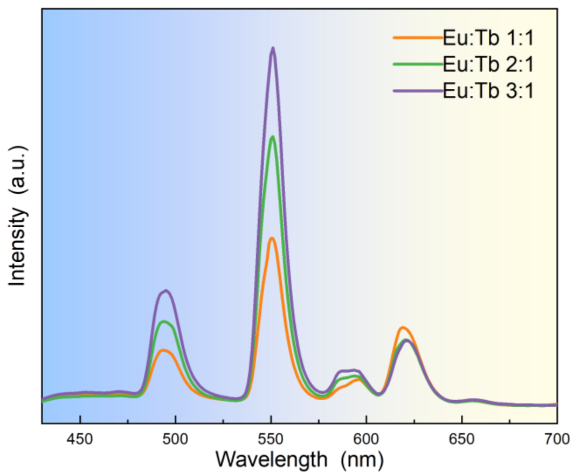

Figure.S5. (Color online)The room-temperature PL spectra of the $Sc_2Mo_3O_{12}$: Eu^{3+}/Tb^{3+} powders

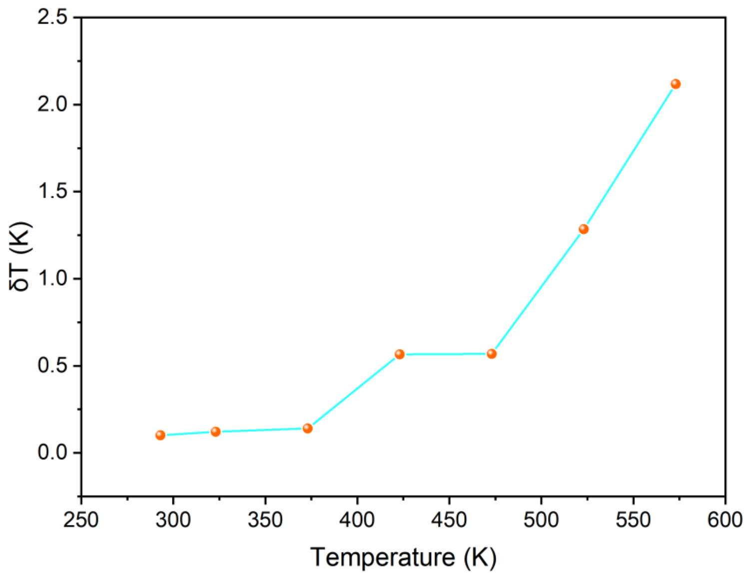

Figure.S6. (Color online) The temperature uncertainties of I_{618}/I_{550}.

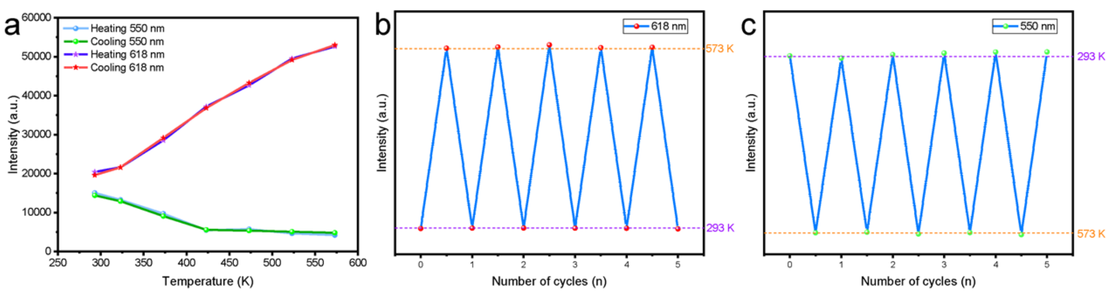

Figure.S7. (Color online)(a) Variation in luminescence intensity at 550 and 618 nm during heating and cooling cycles between 293 and 573 K. And variations in the luminescence intensity of (b) 618 nm and (c) 550 nm during multiple heating and cooling cycles.

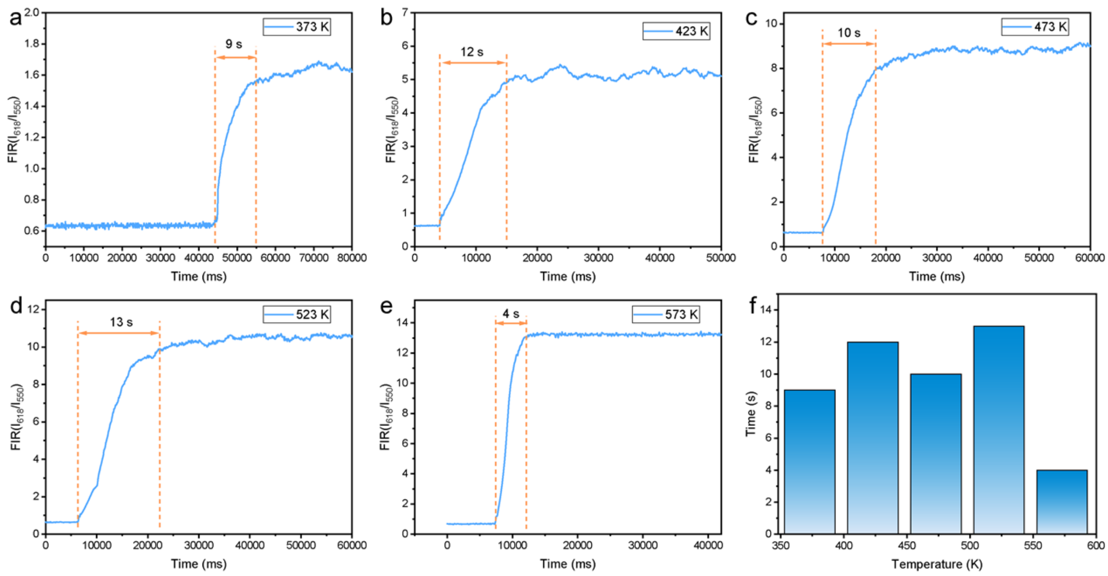

Figure.S8. (Color online)The response time of $Sc_2Mo_3O_{12}:Eu^{3+}/Tb^{3+}$ thin films under conditions of (a) 373 K, (b) 423 K, (c) 473 K, (d) 523 K, and (e) 573 K. (f) Summary of the response times.

Table.S1 The distribution of all elements in the $Sc_2Mo_3O_{12}$: Eu^{3+} sample.

Element	Atomic energy share%	Quality proportion%
O	65.78	28.27
Sc	12.82	15.48
Mo	20.66	53.24
Eu	0.74	3.01

Table.S2 The distribution of all elements in the $Sc_2Mo_3O_{12}$: Tb^{3+} sample.

Element	Atomic energy share%	Quality proportion%
O	69.37	31.67
Sc	11.29	14.48
Mo	18.83	51.55
Tb	0.51	2.30

Table.S3 The distribution of all elements in the $Sc_2Mo_3O_{12}$: Eu^{3+}/Tb^{3+} sample.

Element	Atomic energy share%	Quality proportion%
O	65.50	28.13
Sc	13.12	15.83
Mo	20.79	53.54
Eu	0.23	0.94
Tb	0.37	1.56

Table.S4 Comparison of the performance of temperature sensor and visual temperature sensor.

Compounds	Thermal Expansion	Temperature (K)	Sr (K^{-1})	References
ZrW_2O_8	NTE	523−823	N/A	[1]
$Sc_{1.94}W_3O_{12}$:0.03Dy^{3+}/0.03Tm^{3+}	NTE	298−575	0.71%	[2]
YBO_3: $Bi^{3+}/Eu^{3+}/Tb^{3+}$	PTE	293−473	0.57%	[3]
Y_2O_3: Eu^{3+}/ Tb^{3+}	PTE	330−480	0.68%	[4]
Sr_3MoO_6:Eu^{3+}/Tb^{3+}	NTE	14−300	0.24%	[5]
$Sc_2W_3O_{12}$:Eu^{3+}/Tb^{3+}	NTE	298−473	2.94%	[6]
$Gd_2Mo_3O_{12}$:Eu^{3+}/Tb^{3+}	N/A	80−450	0.5%	[7]
$Lu_2Mo_3O_{12}$:Ho^{3+}/Yb^{3+}	NTE	330−480	0.35%	[8]
Na_2MoO_4:Yb^{3+}/Er^{3+}	NTE/PTE	313−573	3.14%	[9]
Aramid/PVA	NTE/PTE	239−328	N/A	[10]
$Sc_2Mo_3O_{12}$:Eu^{3+}/Tb^{3+}	NTE	293−573	2.35%	This work

Reference

[1] Ding N B, Zhen Y P, Peng R G, et al. Simultaneously preventing oxygen evolution, structure degradation, and thermal release in lithium-rich layered oxides *via in situ* surface anchoring negative thermal expansion material. Adv Energy Mater, 2025: e03693

[2] Huang Z J, Lin J, Zhang X, et al. Fluorescence temperature sensing based on thermal enhancement effect in negative thermal expansion matrix. J Lumin, 2023, 257: 119777

[3] Wu H Y, Li H M, Jiang L H, et al. Design of white-emitting optical temperature sensor based on energy transfer in a Bi^{3+}, Eu^{3+} and Tb^{3+} doped YBO_3 crystal. J Mater Chem C, 2021, 9(23): 7264

[4] Peng L X, Meng Q Y, Sun W J. Size dependent optical temperature sensing properties of Y_2O_3: Tb^{3+}, Eu^{3+} nanophosphors. RSC Adv, 2019, 9(5): 2581

[5] Paiva D V M, Jakka S K, Silva M A S, et al. Investigation on luminescence based optical temperature sensing behavior of Sr_3MoO_6: Eu^{3+}/Tb^{3+}. Optik, 2021, 246: 167825

[6] Fu B, Yan H K, Li R F, et al. Simultaneously tuning the luminescent color and realizing an optical temperature sensor by negative thermal expansion in $Sc_2(WO_4)_3$: Tb/Eu phosphors. Dalton Trans, 2024, 53(2): 798

[7] Han L, Liu J Q, Liu P, et al. Dual-emissive Eu^{3+}, Tb^{3+} Co-doped $Gd_2(MoO_4)_3$ phosphor for optical thermometry application. J Phys Chem Solids, 2021, 153: 110032

[8] Zhang Y X, Chen C H, Wu Y Q, et al. Phonon-assisted thermally enhanced up-conversion fluorescence lifetime thermometry and visualized temperature warning in Yb^{3+}-Ho^{3+}-codoped $Lu_2Mo_3O_{12}$. Inorg Chem, 2025, 64(12): 6205

[9] Zi Y Z, Cun Y K, Bai X, et al. Negative lattice expansion-induced upconversion luminescence thermal enhancement in novel Na_2MoO_4: Yb^{3+}, Er^{3+} transparent glass ceramics for temperature sensing applications. J Mater Chem C, 2023, 11(4): 1541

[10] Sun G F, Ma Z L, Xiao Z, et al. All-fiber-type temperature sensor powered by zinc-ion battery toward wearable sensing clothes for health monitoring. Adv Funct Mater, 2025: e18490